Nanoparticle Self-Assembly of Hierarchically Ordered Microcapsule Structures**

By *Rohit K. Rana*, *Vinit S. Murthy*, *Jie Yu*, and *Michael S. Wong**

As a process by which molecular subunits spatially organize into well-defined supramolecular structures through noncovalent interactions, self-assembly is becoming a powerful synthesis approach for generating advanced materials out of nanoparticle (NP) building blocks.[1] Highly structured NP assemblies, such as wires, rings, and superlattices, can be prepared on flat surfaces.[2] However, ordered NP-based structures remain difficult to prepare in the unsupported colloidal form,[3–5] limiting the prospects of the latter for practical applications (such as drug delivery and catalysis). Here, we identify the solution conditions under which inorganic NPs effectively self-assemble into hierarchically ordered closed-shell structures in the presence of polymer. We demonstrate that in a tandem, two-step process, cationic polyamines form supramolecular aggregates with multivalent counteranions via ionic crosslinking, and negatively charged NPs deposit around these aggregates to form a multilayer-thick shell. The resulting organic/inorganic hybrid microcapsules contain polymer or water in the core interior, depending on the multivalent anion used. In this work, we analyze the polymer aggregation step and present a new preparative route that we term "tandem self-assembly" or "polymer aggregate templating".

Rotello and co-workers showed that appropriately functionalized gold NPs could be induced to self-assemble into micrometer-sized spherical aggregates by using polymer chains specially designed with complementary hydrogen-bonding pendant groups.[4] Stucky and co-workers later showed that diblock copolypeptides could mediate NP self-assembly to form hollow microspheres, in which cysteine and lysine polymer blocks bind to gold and silica NP surfaces, respectively.[5] Hollow-sphere (alternatively, capsule or shell) structures function as encapsulation, protection, and delivery agents, and are used in application areas as diverse as medicine, foods, cosmetics, and paints.[6,7] Further research indicated that Au NP/polymer aggregates were important intermediates in the formation of the hollow spheres.[8] In the course of studying this NP self-assembly process, we observed that poly(L-lysine) (PLL) chains undergo counterion condensation in certain salt solutions to form polymer aggregates, and discovered that these ionically crosslinked polymer aggregates lead to the rapid formation of ordered microcapsule structures.

The room-temperature synthesis of microcapsules (or nanoparticle-assembled capsules, NACs) is illustrated by using PLL conjugated to fluorescein isothiocyanate (FITC) dye. In a typical preparation, 21 μL of an FITC-tagged PLL solution (2 mg mL^{-1}, 68 kDa, HBr salt; 1 Da = 1 g mol^{-1}) was gently mixed for 10 s with 125 μL of a tetrasodium ethylenediamine tetraacetate solution (Na_4EDTA, 4.02 mM) or with a trisodium citrate solution (Na_3Cit, 5.36 mM) (Fig. 1a). The overall charge ratio, R, of total negative charge of the added salt to total positive charge of the polymer ($R = [\text{anion}] \times |z_-| / [\text{polymer}] \times |z_+|$, where z_- is the negative charge per anion and z_+ is the positive charge per chain) was 10. This slightly cloudy polymer/salt solution was aged for 30 min and then vortex mixed with 125 μL of a silica sol (particle diameter, 13 ± 3 nm; 20 wt.-% SiO_2; pH ~ 3.4) for 20 s. The immediate increase in turbidity was due to microcapsule formation. The as-synthesized colloidal assemblies were spherical and had a core/shell morphology with diameters primarily in the 1–4 μm size range, according to optical microscopy images (Figs. 1c,e) and Coulter counter size measurements. The microcapsule yield was estimated on a polymer weight basis from fluorospectroscopy measurements to be 85–90 %. According to thermogravimetric analysis results, the microcapsules had a volatiles content (which includes the salt and polymer) in the 12–15 wt.-% range, indicating that these organic/inorganic NAC materials were composed mostly of silica.

Contrasting the sequential layer-by-layer adsorption of colloidal species around sacrificial templates to yield hollow and filled spheres,[7,9] the above two-step sequence forms the basis of the tandem self-assembly model (Fig. 1a). We followed the process with optical and confocal microscopy using FITC-tagged PLL. The polymer formed globular aggregates upon addition of EDTA (Fig. 1b), which then yielded microcapsule structures (with sharply defined inner and outer perimeters, as observed in Fig. 1c) upon the addition of SiO_2 NPs. The polymer aggregates are necessary for microcapsule formation, as confirmed by a negative control experiment, in which combining SiO_2 NPs with a PLL solution resulted in randomly structured aggregates. The PLL in the microcapsules was located in the core interiors and within the shell walls, where the positively charged polymer chains were interspersed with the negatively charged SiO_2 NPs.

The microcapsules were structurally robust, exhibiting no apparent damage after being subjected to the centrifugation and drying steps used for electron microscopy sample preparation (Figs. 1f–k). Confocal, SEM, and TEM image analysis of the as-synthesized and dried materials indicated contrac-

[*] Prof. M. S. Wong
Department of Chemical and Biomolecular Engineering
Department of Chemistry
Rice University
6100 S. Main Street, Houston, TX 77251-1892 (USA)
E-mail: mswong@rice.edu
Dr. R. K. Rana, V. S. Murthy, J. Yu
Department of Chemical and Biomolecular Engineering
Rice University
6100 S. Main Street, Houston, TX 77251-1892 (USA)

[**] We gratefully acknowledge the financial support of Halliburton Energy Services, the Oak Ridge Associated Universities Ralph E. Powe Junior Faculty Enhancement Award, Kraft Foods, and Rice University. Supporting Information is available online from Wiley InterScience or from the author.

 DOI: 10.1002/adma.200401612

ADVANCED MATERIALS

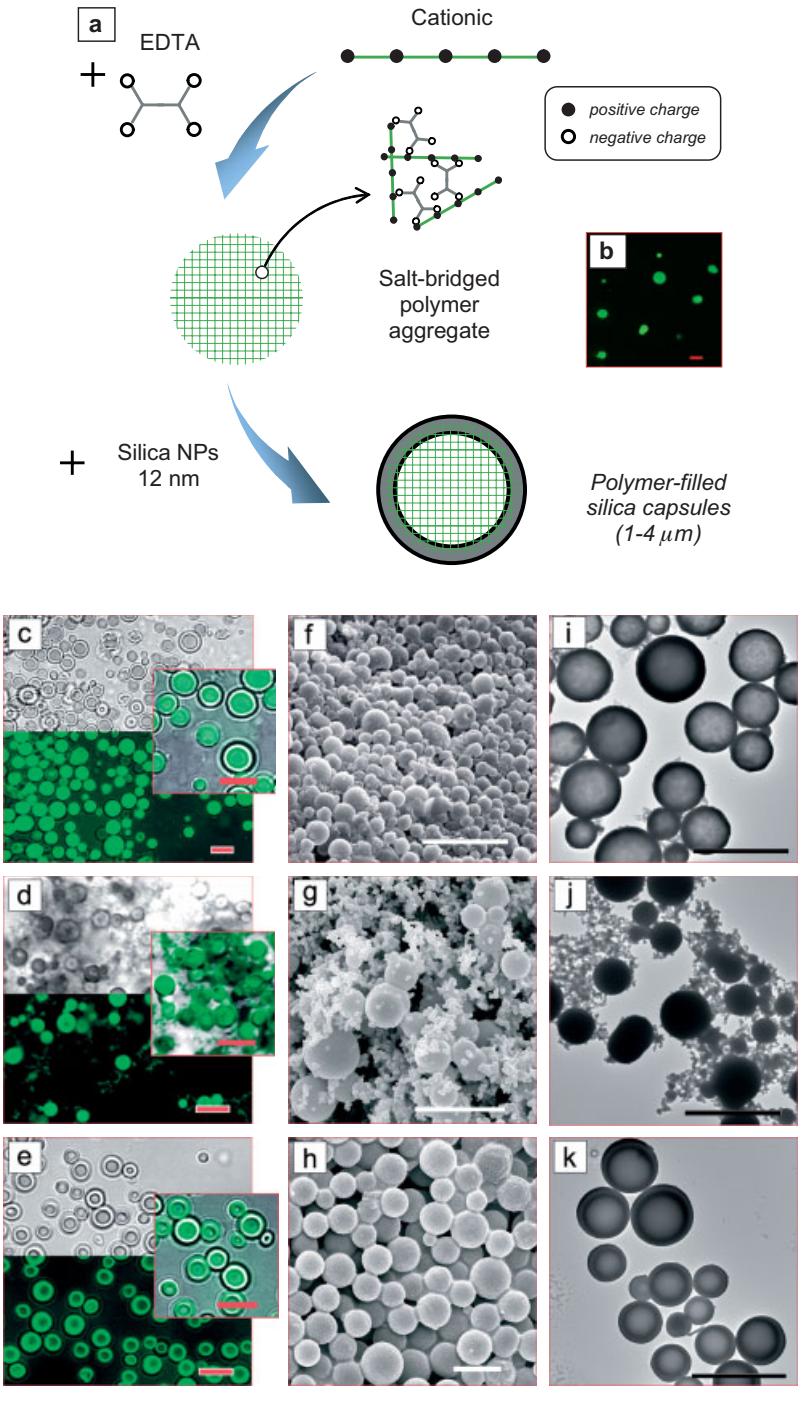

Figure 1. Tandem self-assembly of microcapsules. a) Proposed schematic of the tandem, two-step, formation process, in which positively charged polymer chains ionically crosslink with multivalent anions, and silica NPs subsequently deposit around the polymer aggregates. b) Confocal microscopy image of EDTA-bridged PLL–FITC aggregates. c–e) Bright-field (top), confocal (bottom), and combined confocal/bright-field images (inset) of three different silica structures suspended in water; f–h) scanning electron microscopy (SEM) and i–k) transmission electron microscopy (TEM) images of the corresponding dried structures. Microcapsules in (c,f,i) were self-assembled from SiO_2 NPs, EDTA, and PLL; microspheres in (d,g,j) were synthesized using silicic acid, EDTA, and PLL; microcapsules in (e,h,k) were self-assembled from SiO_2 NPs, citrate, and PLL. All scale bars, 5 μm.

tions of ~20–25 % and ~5–10 % for EDTA-derived and citrate-derived microcapsules, respectively. The former microcapsules had thinner shell walls (~150–200 nm) than the latter (~250 nm), and thus contracted to a greater extent.

The thick microcapsule shell walls are inconsistent with Langmuir-type adsorption of SiO_2 NPs around the polymer aggregates, which should yield shell walls with a thicknesses of one NP (~12 nm). We propose that the NPs penetrate the surface exterior of the polymer aggregate, and that the penetration depth determines the shell thickness, with the implication that smaller particles diffuse deeper into the polymer aggregate than larger particles. Indeed, replacing the SiO_2 particles with oligomeric silicate clusters (~1 nm) in silicic acid preparations led to spheres with thicker shells and even solid silica cores (Figs. 1d,g,j). These particular polymer/silica structures are reminiscent of those reported by the groups of Sumper and Clarson.[10]

The concept of ionic crosslinking between the polymer and salt species provides a simple and informative way of understanding polymer aggregation. The effect of reducing the total number of anion carboxylate groups (negatively charged binding sites) from 4 to 3 can be gauged by replacing EDTA with citrate anions. The citrate anions caused PLL to form aggregates, which also led to the formation of microcapsules after contacting with SiO_2 NPs (Figs. 1e,h,k). Unlike the EDTA-derived materials, however, the polymer in the citrate-derived microcapsules was contained mostly in the shell walls. We speculate that the citrate-bridged PLL aggregate was not as crosslinked (and therefore not as structurally stable) as the EDTA-bridged aggregate, leading to its deaggregation or its collapse after the shell wall was formed. This crosslinking-density argument could explain the observed difference in shell thicknesses; SiO_2 NPs penetrated less deeply into the more-crosslinked EDTA-bridged aggregates, which resulted in thinner shells of the EDTA-derived microcapsules.

The thermodynamically favored formation of carboxylate-ammonium salt bridges drives ionic crosslinking between the multivalent anions and polyamines,[11] but the presence of carboxylate and ammonium groups is an insufficient condition for polymer aggregation. A minimum number of binding sites in the anion is re-

quired, as found for PLL and polyallylamine hydrochloride (PAH) (Supporting Table 1, Supporting Information). Curiously, divalent carboxylate anions (e.g., succinate and malonate) and sulfate anions did not cause PLL to aggregate, but did cause PAH to do so. The aggregation process is apparently sensitive to the molecular structure of the polymer. We found that other polyamines like poly(L-arginine) and polyethyleneimine formed aggregates with citrate anions, as long as the pH of the synthesis medium was below the pK_a of the polyamine (~9.5–11). Aggregation occurred over a wide range of polymer molecular weights (10–250 kDa), with the longer chains tending towards larger polymer aggregates.

The importance of the solution pH to polymer aggregation could be observed by comparing different citrate salts. At the same R ratio, the trisodium and disodium salts led to PLL aggregates (Supporting Table 1, Supporting Information). The pH values of these suspensions were above 5, and acid–base equilibrium calculations indicated that the citrate ion was mostly in the form of $Hcit^{2-}$ and cit^{3-} species. On the other hand, monosodium citrate and citric acid solutions did not yield polymer aggregates, as calculations indicated that the citrate anions were in the form of H_3cit and H_2cit^- species at pH values below 5. Thus, the pH of the solution controls the effective charge (and therefore number of binding sites) of the multivalent anion, and polymer aggregation proceeds within a pH window defined by the pK_a values of the anionic salts and polyamines.

The polymer aggregates, through coalescence, grew in size with time of aging. To gain an understanding of the polymer aggregation dynamics, we focused on citrate-bridged PAH aggregates (Fig. 2a). Aggregate formation was immediate after citrate addition, and the hydrodynamic diameter (D_h) of the PAH solution was measured to be ~110 nm before citrate addition, and ~700 nm 2 min after citrate addition. For comparison, addition of a NaCl solution at the same charge ratio ($R = 10$) and at higher concentrations did not induce PAH ag-

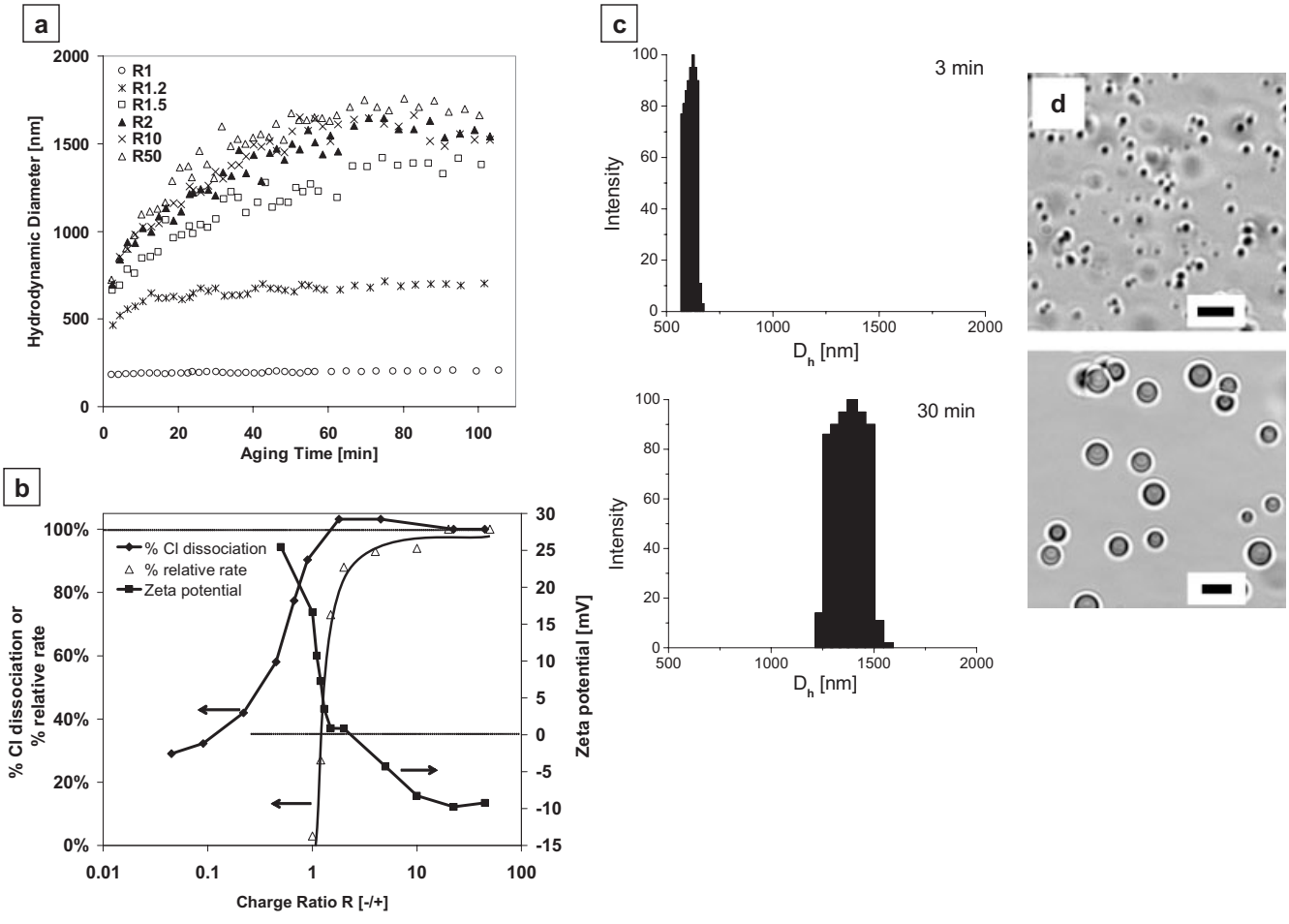

Figure 2. Citrate-bridged PAH aggregates in microcapsule formation. a) Aggregate growth curves of citrate and PAH suspensions at different charge ratios. The charge ratio was adjusted by varying the amount of citrate. The citrate and polymer were combined at time 0. The suspensions could not be analyzed at times earlier than ~2 min due to experimental limitations. b) Aggregate growth rates (at 2 min, determined from growth curves of (a)), zeta potentials, and % dissociation of Cl ions at different values of R. Growth rates were normalized to the maximum growth rate (found at $R = 50$). c) Size distributions of citrate-bridged PAH aggregate ($R = 10$) at 3 min and 30 min. d) Optical microscopy images of microcapsules prepared from corresponding PAH aggregates. Scale bars: 5 μm.

ADVANCED MATERIALS

gregation; instead, PAH contracted ($D_h \sim 30$ nm) due to Coulombic screening of the positively charged ammonium units. Crosslinking between the citrate and the PAH could be tracked by measuring the increase in concentration of free chloride ions caused by the displacement of Cl^- bound to the polymer backbone.[12] Chloride potentiometric measurements of the PAH-only solution indicated that 26 % of the total Cl^- was dissociated, and that one citrate molecule displaced ~2.2 Cl ions, based on the initial slope of the Cl dissociation curve (Fig. 2b). Although the polymer aggregates were metastable, they were apparently rigid, and allowed for NP deposition and shell formation; the addition of SiO_2 NPs to the aggregate suspension aged at different times resulted in microcapsules with tunable diameters (Figs. 2c,d).

The charge ratio governs the formation and growth rate of the salt-bridged polymer aggregates, which can be rationalized using the Derjaguin–Landau–Vervey–Overbeek (DLVO) theory of colloidal stability[13]—namely, a suspension of charged colloidal particles is kinetically stable to aggregation if the particle surfaces are sufficiently charged to repel each another. Polymer aggregation occurs at $R > 1$, which is coincident with the near-complete removal of Cl^- from the PAH by the citrate anions (Fig. 2b). The zeta potentials (ζ) of the polymer aggregates decrease in magnitude and eventually assume negative values with increasing R values; the observed charge reversal results from citrate anions binding to the aggregate exterior. The aggregates remained insufficiently charged ($-10\ \text{mV} < \zeta < +10\ \text{mV}$, between $R = 1.2$ and $R = 50$), allowing for fast aggregate growth and for contact with SiO_2 NPs leading to shell formation.

We have found the concept of tandem self-assembly of charged nanoparticles and polymer molecules to be broadly applicable. NPs of other metal oxides, such as tin oxide and zinc oxide, can be used to generate capsular structures as long the particle surface is negatively charged under the synthesis conditions (Supporting Table 2, Supporting Information). This condition is ensured if the pH of the suspending fluid is higher than the point of zero charge of the metal oxide.[13] Other NPs with negatively charged surface species, such as citrate-stabilized CdSe and carboxylated polystyrene beads, can also be used to make microcapsules. Interestingly, negatively charged linear polyelectrolytes, like poly(acrylic acid) and poly(styrene sulfonic acid), can also yield microcapsular structures, in which they presumably take the place of silica NPs in the shell formation step (images are not shown for brevity). Polymer aggregates can also be supported on surfaces to template the formation of capsular hybrid structures (Figure, Supporting Information). Citrate-bridged PAH aggregates adsorbed onto a mica surface appear as flattened spheres due to spreading, and lead to dome-like shells after contacting with SiO_2 NPs.

The rapid generation of microcapsules in an aqueous medium is amenable to the facile encapsulation of water-soluble compounds, for example, by adding a solution of the desired compound to a PLL/citrate suspension prior to adding the silica sol. To test the feasibility of microcapsules as reaction vessels,[14] we encapsulated the enzyme, acid phosphatase, at a loading of 0.15 mg/(mg microshell) and suspended the spheres in a solution containing fluorescein diphosphate, a non-fluorescent molecule. Fluorescence emerged and grew in intensity inside the microcapsule and within the shell walls over a course of 40 min, due to the formation of fluorescein from enzymatic cleavage of the phosphate groups (Fig. 3). We could not discern if the enzyme molecules were located inside the microcapsules, within the shell walls, or both, but confocal analysis clearly indicated that the generated fluorescein accumulated inside the shell walls and in the capsules' interiors, before diffusing out after 15 min. Vigorous mixing or sonication did not noticeably degrade the microcapsule structure or the contained enzyme. The microcapsules allow the confined enzymes to function in a protected environment, and allow the reactant and product molecules to transport across the permeable shell walls.

In conclusion, we demonstrate that electrostatic interactions at the molecular and nanometer levels can be employed in the self-assembly of highly structured, nanoparticulate-based materials. Under solution conditions that favor the appropriate acid–base and colloidal chemical interactions, nanometer-sized particles organize into multiscale-ordered ensembles in the form of micrometer-sized spheres with submicrometer thick shells. This form of materials synthesis involves the simple mixing of well-defined precursors, and thus scale-up of the materials is readily accomplished. The self-assembly chemistry is very flexible, and can be extended to different NP compositions, polymer molecules, and multivalent anions. The ease of encapsulation, the mild conditions of microcapsule synthesis, and the structural robustness and semipermeability of the organic/inorganic shell wall, collectively point to the exciting possibilities of microcapsules and surface-patterned microcapsule arrays as controlled release devices and reaction vessels.

Experimental

Materials: FITC-tagged poly(L-lysine hydrobromide) (68 kDa), poly(L-lysine hydrobromide) (30 and 222 kDa), poly(L-arginine) (94 kDa), poly(allylamine hydrochloride) (15 and 70 kDa), branched polyethyleneimine (750 kDa), poly(sodium 4-styrenesulfonic acid) (PSS, 70 kDa), Poly(acrylic acid, sodium salt) (PAA, 30 kDa, 40 wt.-% in water), all the salts, and the EDTA buffer solution (2 mM EDTA, pH 8.4) were procured from Sigma-Aldrich (USA) and used as received. All solutions were prepared using de-ionized water (18.2 MΩ, Barnstead NANOpure Diamond water purification system). SiO_2 NPs (Snowtex-O, 13 ± 3 nm, 20 wt.-% SiO_2, pH 3.4) were obtained from Nissan Chemical (USA). ZnO (DP5370, 50–90 nm, 30 wt.-% containing 4 wt.-% of PAA salt, pH 9.5), and SnO_2 (SN15, 10–15 nm, 15 wt.-%, pH 10) were purchased from Nyacol Nanotechnologies (USA) and used after dilution in water. Citrate-stabilized CdSe NPs (3–5 nm) were synthesized in an aqueous medium by the reaction of cadmium nitrate with selenourea. Carboxylated polystyrene NPs tagged with FITC were obtained from Molecular Probes, Inc. (USA).

Synthesis of SiO_2 Microcapsules: In all the preparations, 21 μL of an aqueous polymer solution (2 mg mL^{-1}) was gently mixed for 10 s with 125 μL of a salt solution (Na_4EDTA or Na_3Cit). The overall charge ratio was varied from 0.5 to 100 by adding the same volume of

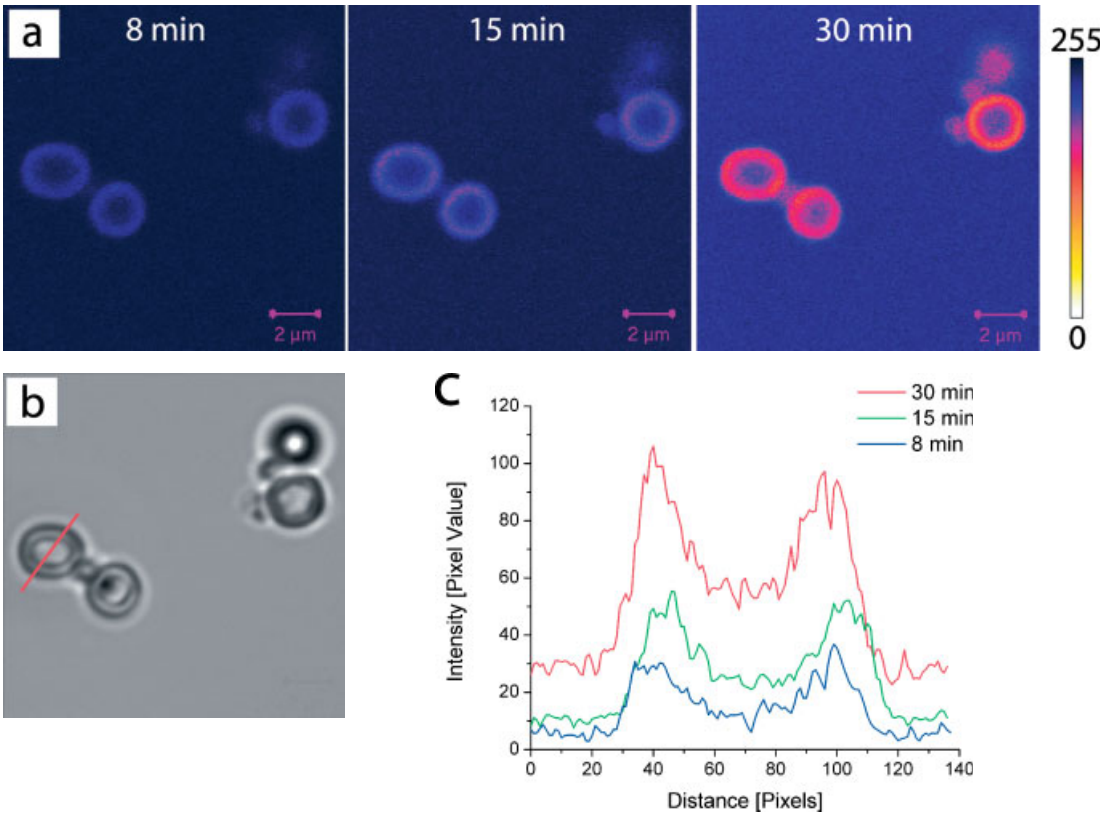

Figure 3. Representative microcapsules prepared from citrate-bridged PLL aggregates and SiO_2 NPs that contained the enzyme, acid phosphatase, in an aqueous solution containing fluorescein diphosphate: a) a series of time-lapse confocal microscopy images collected over the course of 30 min, b) bright-field image, and c) line intensity profiles along the red line shown in (b). The reactant diffuses inside the microcapsules and interacts with the encapsulated enzyme to form the fluorescent fluorescein product. Scale bars: 2 μm.

varying salt concentration to maintain a constant polymer concentration. The polymer/salt solution was aged for different times (2–30 min) and then vortex mixed with 125 μL of a silica sol for 20 s. The resultant silica microcapsules were aged for 2 h and then centrifuged, decanted, and resuspended in EDTA buffer for further characterization.

Synthesis of SiO_2 Solid Spheres: Silicic acid, with a nominal composition of $Si(OH)_4$, was prepared to a 1 M concentration by dissolving tetramethyl orthosilicate in a 10^{-3} M HCl solution and used within 1 h. Silica spheres were obtained by mixing 125 μL of silicic acid with the above polymer-aggregate suspension for 10 s. The resultant silica spheres were immediately centrifuged, decanted, and resuspended in water.

Synthesis of Microcapsules from Other NPs: Microcapsule synthesis from various NPs and polyamines was carried out as follows: 21 μL of an FITC-tagged PLL or PAH solution (2 mg mL^{-1}) was mixed with 125 μL of a Na_3Cit solution ($R = 10$) and aged for 30 min. To this polymer/salt suspension was added different NPs or anionic polymers with the following volumes and concentrations, respectively: SiO_2 (Snowtex-O, 125 μL, 20 wt.-% solids); ZnO (125 μL, 1 wt.-%); SnO_2 (125 μL, 5 wt.-%); CdSe (125 μL, 5 μM); carboxylated polystyrene (100 μL, 0.01 wt.-%); PAA (30 μL, 5.0 wt.-%); PSS (30 μL, 3.0 wt.-%).

Enzyme Encapsulation and Testing: 10 μL of a solution of the acid phosphatase enzyme (7.5 mg mL^{-1} = 40.2 units mL^{-1} in EDTA buffer, pH 8.4) was added to a citrate/PLL suspension ($R = 10$), which was prepared by mixing 21 μL of PLL (2 mg mL^{-1}, 222 kDa) and 125 μL of Na_3Cit (5.36 mM), and aged for 20 min. The reaction suspension was aged for 10 min before SiO_2 NPs were added, and thoroughly mixed. The resulting microcapsule suspension was centrifuged and rinsed with EDTA buffer several times, to ensure removal of any free enzymes. Enzyme loading of the microcapsules was determined by assaying the catalytic activity of the free enzyme in the wash. An encapsulation efficiency of 60 % was estimated. 5 μL of 0.1 mM fluorescein diphosphate solution was added to the washed microcapsules, and the reaction mixture was imaged via confocal microscopy.

Characterization Techniques: The structures were characterized in the wet state via bright-field optical microscopy (Carl Zeiss Axioplan2 and Nikon Eclipse E600), laser-scanning confocal microscopy (Carl Zeiss, LSM 510 Meta), fluorescence spectroscopy (Jobin-Yvon Horiba Fluoromax 3 spectrophotometer), and Coulter counter measurements (Beckman Coulter, Multisizer 3). In the dry state, the structures were analyzed via transmission electron microscopy (JEM 2010 FasTEM), scanning electron microscopy (JEOL6500), and thermogravimetric analysis (TA Instruments, SDT 2960). Tapping mode AFM was performed on a Digital Instruments Nanoscope IIIA atomic force microscope using a 125 micrometer etched single crystal silicon probe (TESP) tip. Dynamic light scattering and zeta potential analysis were carried out with a Brookhaven Instruments ZetaPALS with BI-9000AT digital autocorrelator. Zeta potentials were calculated from electrophoretic mobility measurements using Henry's equation (for NPs) and Smoluchowski's equation for polymer aggregates.

Received: October 1, 2004
Final version: December 14, 2004

ADVANCED MATERIALS

[1] a) S. Mann, G. A. Ozin, *Nature* **1996**, *382*, 313. b) G. M. Whitesides, M. Boncheva, *Proc. Natl. Acad. Sci. USA* **2002**, *99*, 4769. c) R. Shenhar, V. M. Rotello, *Acc. Chem. Res.* **2003**, *36*, 549. d) A. L. Rogach, *Angew. Chem. Int. Ed.* **2003**, *43*, 148. e) M. P. Pileni, *Langmuir* **1997**, *13*, 3266.

[2] a) C. B. Murray, C. R. Kagan, M. G. Bawendi, *Science* **1995**, *270*, 1335. b) H. Zeng, J. Li, J. P. Liu, Z. L. Wang, S. H. Sun, *Nature* **2002**, *420*, 395. c) M. Kimura, S. Kobayashi, T. Kuroda, K. Hanabusa, H. Shirai, *Adv. Mater.* **2004**, *16*, 335. d) H. Y. Li, S. H. Park, J. H. Reif, T. H. LaBean, H. Yan, *J. Am. Chem. Soc.* **2004**, *126*, 418. e) P. Moriarty, M. D. R. Taylor, M. Brust, *Phys. Rev. Lett.* **2002**, *89*, 248. f) W. A. Lopes, H. M. Jaeger, *Nature* **2001**, *414*, 735. g) S. W. Lee, S. K. Lee, A. M. Belcher, *Adv. Mater.* **2003**, *15*, 689. h) R. A. McMillan, C. D. Paavola, J. Howard, S. L. Chan, N. J. Zaluzec, J. D. Trent, *Nat. Mater.* **2002**, *1*, 247. i) J. A. Theobald, N. S. Oxtoby, M. A. Phillips, N. R. Champness, *Nature* **2003**, *424*, 1029. j) F. X. Redl, K. S. Cho, C. B. Murray, S. O'Brien, *Nature* **2003**, *423*, 968. k) E. Rabani, D. R. Reichman, P. L. Geissler, L. E. Brus, *Nature* **2003**, *426*, 271. l) S. L. Tripp, S. V. Pusztay, A. E. Ribbe, A. Wei, *J. Am. Chem. Soc.* **2002**, *124*, 7914. m) T. Hassenkam, K. Norgaard, L. Iversen, C. J. Kiely, M. Brust, T. Bjornholm, *Adv. Mater.* **2002**, *14*, 1126.

[3] a) C. A. Mirkin, R. L. Letsinger, R. C. Mucic, J. J. Storhoff, *Nature* **1996**, *382*, 607. b) J. P. Novak, D. L. Feldheim, *J. Am. Chem. Soc.* **2000**, *122*, 3979. c) Z. Y. Tang, N. A. Kotov, M. Giersig, *Science* **2002**, *297*, 237. d) T. Yonezawa, H. Matsune, N. Kimizuka, *Adv. Mater.* **2003**, *15*, 499.

[4] A. K. Boal, F. Ilhan, J. E. DeRouchey, T. Thurn-Albrecht, T. P. Russell, V. M. Rotello, *Nature* **2000**, *404*, 746.

[5] M. S. Wong, J. N. Cha, K. S. Choi, T. J. Deming, G. D. Stucky, *Nano Lett.* **2002**, *2*, 583.

[6] *Mater. Res. Soc. Symp. Proc.* (Eds: D. L. Wilcox, Sr., M. Berg, T. Bernat, D. Kellerman, J. K. Cochran, Jr.), Materials Research Society, Pittsburgh, PA **1995**, Vol. 372.

[7] F. Caruso, *Chem.—Eur. J.* **2000**, *6*, 413.

[8] a) J. N. Cha, H. Birkedal, L. E. Euliss, M. H. Bartl, M. S. Wong, T. J. Deming, G. D. Stucky, *J. Am. Chem. Soc.* **2003**, *125*, 8285. b) V. S. Murthy, J. N. Cha, G. D. Stucky, M. S. Wong, *J. Am. Chem. Soc.* **2004**, *126*, 5292.

[9] F. Caruso, R. A. Caruso, H. Möhwald, *Science* **1998**, *282*, 1111.

[10] a) N. Kröger, S. Lorenz, E. Brunner, M. Sumper, *Science* **2002**, *298*, 584. b) M. Sumper, S. Lorenz, E. Brunner, *Angew. Chem. Int. Ed.* **2003**, *42*, 5192. c) S. V. Patwardhan, N. Mukherjee, M. Steinitz-Kannan, S. J. Clarson, *Chem. Commun.* **2003**, 1122.

[11] a) H. R. Bosshard, D. N. Marti, I. Jelesarov, *J. Mol. Recognit.* **2004**, *17*, 1. b) C. De Stefano, C. Foti, O. Giuffre, S. Sammartano, *J. Chem. Eng. Data* **2001**, *46*, 1417.

[12] K. S. Schmitz, *Macroions in Solution and Colloidal Suspension*, VCH, Weinheim, Germany **1993**. Counterion condensation occurs to neutralize a percentage of the ionizable side groups of the repeat units, such that the average distance between the charged groups (l_B, Bjerrum length) is sufficiently large to reduce the electrostatic interaction potential between the like-charged groups down to thermal energy levels ($e^2/\varepsilon l_B \sim kT$; e: electron charge, ε: dielectric constant; k: Boltzmann's constant; T: temperature).

[13] R. J. Hunter, *Foundations of Colloid Science*, 3rd ed., Oxford University Press, New York **2001**.

[14] a) P. Walde, S. Ichikawa, *Biomol. Eng.* **2001**, *18*, 143. b) C. Y. Gao, E. Donath, H. Möhwald, J. C. Shen, *Angew. Chem. Int. Ed.* **2002**, *41*, 3789.

Cholesteric Emulsions for Colored Displays

By *Giovanni De Filpo*,* *Fiore P. Nicoletta*, and *Giuseppe Chidichimo*

Cholesteric liquid crystals (LCs) have a helical texture that selectively reflects a specific wavelength of light associated with the cholesteric LC helical pitch when light propagates parallel to the helical axis.[1] This characteristic is attractive for reflective color-display devices without the need for backlighting, polarizers, or color filters.

In the past it has been demonstrated that polymer-dispersed cholesteric liquid crystals (PDCLCs) can be used in electro-optical color displays.[2–5] In the PDCLC displays, low-molecular-weight chiral nematic materials are dispersed in a non-mesogenic polymer. Usually, to obtain a cholesteric colored display it is necessary to create separate sealed compartments, where each compartment contains a cholesteric liquid crystal having a pitch length that effectively reflects a different primary color, i.e., red, green, and blue. There are many ways to control the cholesteric pitch: by varying the temperature of the cholesteric LC phase,[1] by adding different amounts of the chiral agent in the LC phase,[6] or by using phototunable chiral compounds embedded in the liquid crystals.[7–9] This last method provides the three primary colors in a sequential array from the same original cholesteric stock solution constituted from a mixture of the nematic host, a chiral dopant, and a tunable chiral material, i.e., a chiral compound in which the chiral center is linked to a photosensitive group.

This photosensitive chiral material, whose chirality is adjustable by UV irradiation, enables adjustment of the pitch of the cholesteric material, thereby producing the three reflected colors for a multicolor reflective color display. Vicentini et al.[7] described a multicolor reflective cholesteric display obtained by using a phototunable chiral material linked to the polymer network. In this way they solved the problem of color diffusion due to the spontaneous migration of the phototunable molecules by creating consecutive arrays at different phototunable chiral material concentrations.

We present a new colored cholesteric display obtained by oriented cholesteric LC molecules confined in elliptic droplets dispersed in an organic-monomer matrix. It is well-known that LC emulsions in organic monomers are stable over long times and require low driving electric fields in comparison to traditional PDCLCs due to the small anchoring energy of the LC in the droplets.[10,11] The cholesteric LC pitch has been adjusted by using a photosensitive chiral material in order to produce the three reflected colors (red, green, and blue) for a

[*] Dr. G. De Filpo, Prof. F. P. Nicoletta, Prof. G. Chidichimo
Department of Chemistry, University of Calabria
Arcavacata di Rende I-87036 (CS) (Italy)
E-mail: defilpo@unical.it

  DOI: 10.1002/adma.200401912